



# Comparative analysis of accidental sequences with conventional and Accident Tolerant Fuels (ATF) in VVER-1000 reactors

Elena Redondo-Valero <sup>a</sup> , Cesar Queral <sup>a,\*</sup> , Kevin Fernandez-Cosials <sup>a</sup> ,  
Jorge Sanchez-Torrijos <sup>b</sup> , David Canal <sup>a</sup> , Emilio Castro-Gonzalez <sup>a</sup> ,  
Victor Hugo Sanchez-Espinoza <sup>c</sup> 

<sup>a</sup> Universidad Politécnica de Madrid (UPM), Ramiro de Maeztu 7, 28040 Madrid, Spain

<sup>b</sup> NFQ Advisory Services S.L., O'Donnell 34, 28009 Madrid, Spain

<sup>c</sup> Karlsruhe Institute of Technology (KIT), Hermann-von-Helmholtz-Platz 1, 76344 Eggenstein-Leopoldshafen, Germany

## ARTICLE INFO

### Keywords:

VVER-1000  
FeCrAl  
Cr-Coating Zry  
ATF  
TRACE

## ABSTRACT

A significant percentage of reactors in operation, under construction or recently commissioned are VVER reactors. In parallel, there is a growing interest in analyzing the behavior of Accident Tolerant Fuels (ATF), also known as Advanced Technology Fuels, under development in different nuclear reactor designs. Among the new ATF designs, the FeCrAl and Cr-coated Zircaloy claddings are one of the most currently studied. In addition to having a relatively high level of technology readiness, these evolutionary cladding materials offer an improved resistance to oxidation and hydrogen absorption, as well as improved mechanical strength. All these properties are essential in accident sequences where high core temperatures are reached. In the present study, core damage sequences have been analyzed with a model of a VVER-1000 reactor for the TRACE system code. The results indicate that for certain sequences, such as a Small Break Loss of Coolant Accident (SBLOCA) or an Station Blackout (SBO), these new cladding materials increase the reactor safety margins by extending the time available to recover the safety systems involved in core cooling and replenishment of the reactor coolant system inventory.

## 1. Introduction

VVER-1000 are four-loop Pressurized Water Reactors (PWR). They have consistently featured horizontal Steam Generators (SGs), which provide a larger coolant inventory compared to western PWRs. Another key feature is their use of hexagonal Fuel Assemblies (FA) together with a tighter triangular FA arrangement. Many countries either operate VVERs or are considering them as part of their energy strategy (Queral et al., 2021).

Advanced Technology Fuel (ATF), formerly known as Accident Tolerant Fuel, have attracted considerable interest in the nuclear industry for their potential to improve reactor safety. The development of ATFs aims to improve the performance of nuclear fuels in high temperature scenarios. This advancement is critical to extending the safety margins of nuclear reactors, reducing the likelihood of Core Damage (CD) and providing additional time for safety systems in the event of an accident. Additionally, ATFs offers advantages for flexible operation, allowing reactors to adapt more efficiently to load-following conditions,

which are becoming increasingly important in modern energy grids (Doncel et al., 2024; Zhang et al., 2014).

Among the various ATF designs, FeCrAl and Cr-coated Zircaloy (Zry) claddings are the most promising short-term alternatives to conventional Zry cladding (Yue et al., 2020) (E110 for the VVER-1000 reactors). FeCrAl cladding, made with an iron-chromium-aluminum alloy, exhibits improved resistance to oxidation in comparison to the conventional Zry claddings during, for example, LOCA sequences (Sanchez-Torrijos, 2024). This resistance would be particularly valuable during accidents where Zry cladding can oxidize rapidly leading to significant hydrogen generation. Similarly, Cr-coated Zry claddings, which consist of a thin chromium layer deposited on a conventional zirconium cladding, provide enhanced oxidation resistance and reduced hydrogen production under high-temperature conditions. Both materials can help to mitigate the risks associated with the metal-water reaction, which generates heat and hydrogen that, when mixed with oxygen, poses a deflagration hazard (Doncel et al., 2024).

In this study, several accidental sequences have been simulated for a VVER-1000 reactor, considering FeCrAl and Cr-coated Zry as cladding

\* Corresponding author.

E-mail address: [cesar.queral@upm.es](mailto:cesar.queral@upm.es) (C. Queral).

<https://doi.org/10.1016/j.nucengdes.2025.114591>

Received 18 August 2025; Received in revised form 31 October 2025; Accepted 4 November 2025

Available online 10 November 2025

0029-5493/© 2025 The Author(s). Published by Elsevier B.V. This is an open access article under the CC BY-NC-ND license (<http://creativecommons.org/licenses/by-nc-nd/4.0/>).

## Nomenclature

AFW	Auxiliary Feed Water
ATF	Advanced Technology Fuels
BRU-A	Steam Dump Valves to the Atmosphere
BRU-K	Steam Dump Valves to the Condenser
BRU-SN	Steam Dump Valves to the Atmosphere
CD	Core Damage
CL	Cold Leg
DC	Damage Curve
DEGB	Double Ended Guillotine Break
EBIS	Emergency Boron Injection System
ECCS	Emergency Core Cooling System
EFW	Emergency Feed Water
FA	Fuel Assembly
HA-1	First Stage Hydroaccumulator
HL	Hot Leg
HPIS	High Pressure Injection System

LBLOCA	Large Break Loss of Coolant Accident
LPIS	Low Pressure Injection System
MFW	Main Feed Water
MSIV	Main Steam Isolation Valve
NPP	Nuclear Power Plant
PCT	Peak Cladding Temperature
PRZ	Pressurizer
PWR	Pressure Water Reactor
RCP	Reactor Coolant Pump
RCS	Reactor Coolant System
RPV	Reactor Pressure Vessel
SBLOCA	Small Break Loss of Coolant Accident
SBO	Station Blackout
SC	Success Criteria
SG	Steam Generator
SL	Steam Line
Zry	Zircaloy

materials. The simulations have been performed by means of a VVER-1000 model for the TRACE5P6 system code. As TRACE5P6 does not support ATF materials by default (Sanchez-Torrijos et al., 2024), modified versions of the code developed by the UPM and NFQ working groups have been used for this analysis.

The paper is structured as follows; an initial introduction has been presented. Then, the modifications performed in the TRACE5P6 system code for ATF cladding materials are described in Section 2. Section 3 shows the VVER-1000 TRACE model applied in the following analyses. Thereafter, Sections 4, 5 and 6 present the analyses performed for different sequences like SBO (Section 4), LBLOCA (Section 5) and SBLOCA (Section 6). Subsequently, in Section 7, the results of the increase of available time due to the use of different ATF materials in the different accidental sequences (SBO, LBLOCA and SBLOCA) are compared. Finally, the conclusions are presented in Section 8.

## 2. Modifications of the TRACE5P6 system code for ATF cladding Materials: FeCrAl and Cr-Coated Zry

As previously stated in the introduction, two in-house versions of the TRACE5P6 system code have been developed and specifically adapted to model both types of cladding under analysis: FeCrAl and Cr-coated Zry. In order to ensure accurate implementation of the ATF cladding, a comprehensive review of publicly available data has been undertaken. This process has enabled the selection of the most relevant models and properties, which have then been integrated into the in-house versions of the TRACE code following a specific approach for each type of cladding, see Fig. 1:

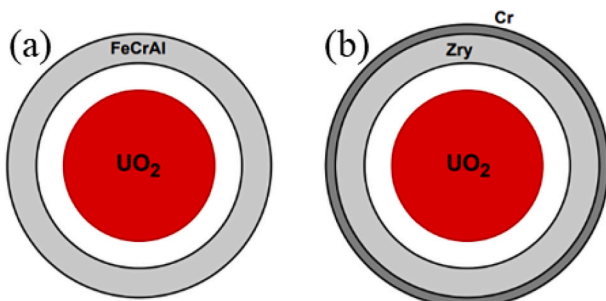


Fig. 1. Modelling of fuel rods: a) FeCrAl, b) Cr-coated Zry.

- E-110. The modeling of this material is intrinsic to the TRACE code, as the corresponding material properties and thermomechanical models are already available. Cladding Thickness: 570  $\mu\text{m}$ .
- Considering the FeCrAl material, the correlations for the material physical properties along with the mechanical and corrosion models were implemented in TRACE5P6 system code (Field et al., 2018; IAEA, 2020; Wu and Shirvan, 2020). These properties and models include the density, the oxidation rate, the Young modulus, the high-temperature creep strain, the poison's ratio, the burst stress criterion, the yield stress, the ultimate tensile strength, the thermal expansion coefficient and the thermal conductivity (Sanchez-Torrijos, 2024). Besides, a thickness of 309  $\mu\text{m}$  was assumed, a reduction obtained by neutron economy considerations.
- In the case of the Cr-coated Zry cladding, the possibility of the TRACE5P6 system code to consider a cladding consisting of different material layers has been used (Canal et al., 2025). Since the thickness of the Cr coating is very small, in the order of 25  $\mu\text{m}$ , it has been assumed that the thermo-mechanical behavior of the Cr-coated Zry cladding would be comparable to that of an uncoated E110 cladding.

Besides, oxidation models corresponding to FeCrAl-MIT and Cr-coated Zry, describing the oxidation kinetics of these materials under high temperature conditions were considered, see Fig. 2.

In addition to taking into consideration the oxidation models, the

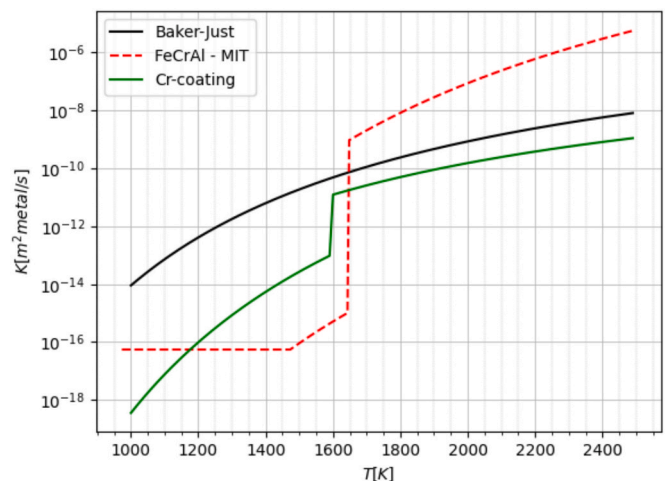


Fig. 2. Parabolic oxidation rate for different cladding materials.

values for each ATF cladding material for the heat of the reaction were also incorporated into the TRACE code to ensure that the high-temperature oxidation phenomena impact on the calculation results was properly captured. Specifically, a value of 12.45 MJ/kg is used for FeCrAl and a 4.327 MJ/kg for the Cr-coating. Besides, it should be noted that the acceptance criterion (AC) considered for the E110 cladding is the classical Zry embrittlement value, 1477 K, but for the FeCrAl and the Cr-coated Zry claddings there is still no consensus on which AC should be used in safety analyses:

- For the FeCrAl material two values are under discussion, 1477 K as for the Zry or 1773 K, which is the melting point of the FeCrAl alloy (Baker et al., 2024).
- For the Cr-coated Zry cladding, the situation is more complex, as the behavior of the Cr layer and its interaction with the underlying Zry needs to be considered. The Cr-coated Zry AC can be assumed to be 1605.15 K, which is the eutectic reaction temperature between the Zr and Cr. Above this threshold, the formation of an eutectic liquid phase could compromise the integrity of the coating, potentially accelerating oxidation and leading to structural degradation (Aragon et al., 2025; Brachet et al., 2020).

It should also be noted that the available experimental data on these new materials is limited, meaning that the AC values used by different studies may vary.

### 3. VVER-1000 TRACE model incorporating ATF

The TRACE5P6 model for the primary and secondary side including safety and some control systems is built from the VVER-1000 RELAP5 model used in (Sanchez-Espinoza and Bottcher, 2006), see Fig. 3 and Fig. 4. This model has been applied for LOCA and SBO analyses in

previous studies, see (Redondo-Valero et al., 2023a; Redondo-Valero et al., 2023b; Redondo-Valero et al., 2024; Redondo-Valero et al., 2025). The resulting integral plant model consists of the following elements:

- Primary loops: Cold Legs (CLs), Hot Legs (HLs) and Reactor Coolant Pumps (RCPs).
- Pressurizer (PZR): connected to HL 4 by the surge line. It contains spray lines, attached to the CL 1, three safety valves and four groups of heaters.
- Reactor Pressure Vessel (RPV): it has been modelled by a 3D VESSEL component which is divided into 50 axial nodes, 6 azimuthal sectors and 6 radial sectors. In the core region, the three internal rings model the core whereas the fourth ring is dedicated to bypass. The core barrel is modelled by the fifth ring and the downcomer by the sixth.
- SGs: In the primary side, the SG-tubes are modelled by three horizontal pipes. In the secondary side, the heat transfer zone is simulated with three horizontal levels and the liquid/steam SEPARATOR component placed in the upper part.
- Steam lines (SL): including one steam dump valve to the atmosphere (BRU-A), two safety valves, one main isolation valve (MSIV) and a check valve in each SL.
- Steam header: containing steam dump valves to the condenser (BRU-K), steam dump valves to the atmosphere (BRU-SN) and the turbine connection.

The Emergency Core Cooling System (ECCS) is represented by four first Stage Hydro-accumulators (HA-1), two of them are connected to the reactor upper plenum and two others are connected to the downcomer, three Low Pressure Injection System (LPIS) trains and three HPIS trains. The Main Feed Water (MFW) and the Emergency Feed Water (EFW) are also included in the model as boundary conditions.

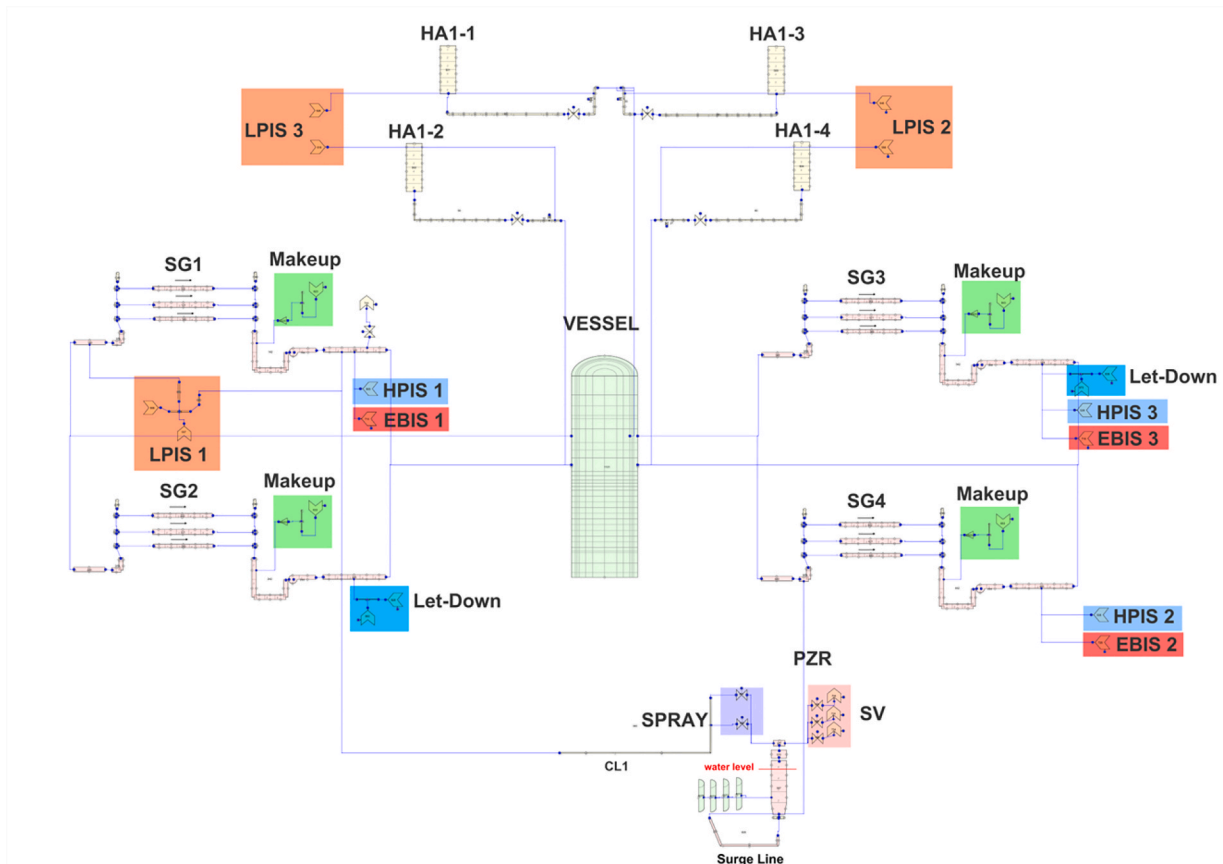


Fig. 3. VVER-1000/V320 RCS TRACE5P6 model.

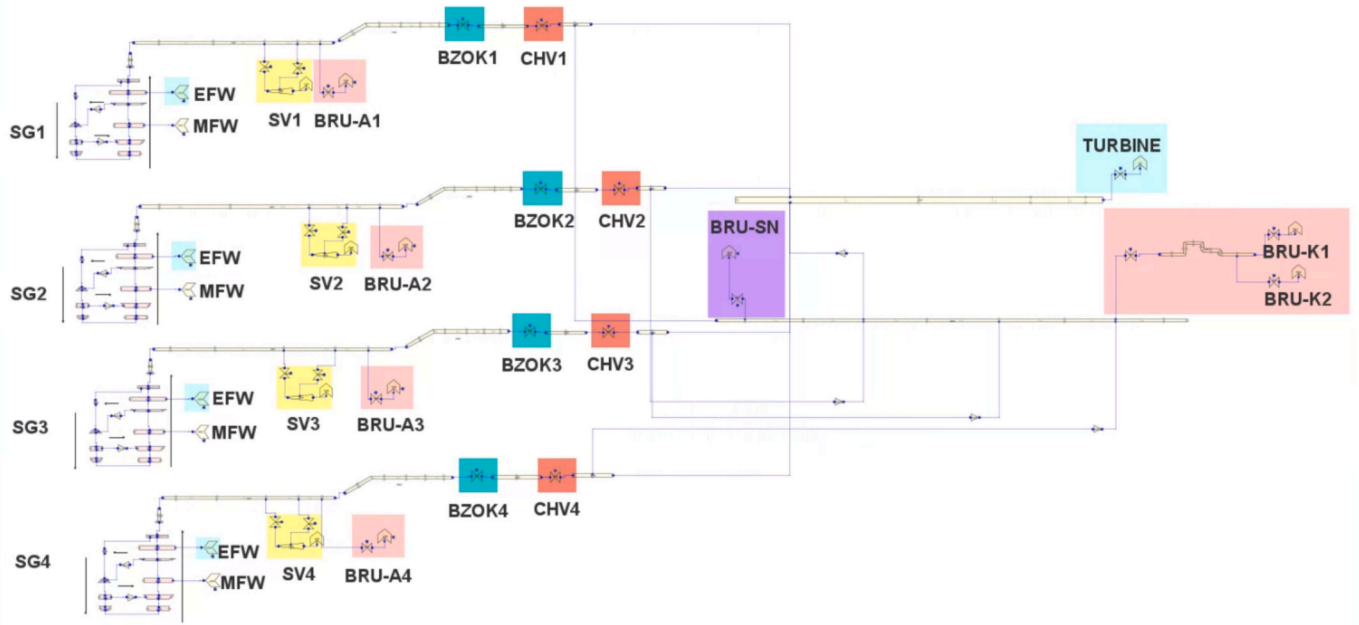


Fig. 4. VVER-1000/V320 Secondary Side TRACE5P6 model.

Regarding the modelling of fuel rods containing FeCrAl, given that the neutron capture cross-section of FeCrAl is much larger than that of E110, it is proposed that the cladding thickness be reduced by 0.185 mm, in line with other studies on Westinghouse PWR, see (Sanchez-Torrijos, 2024). This has been achieved by increasing the internal radius of the cladding while maintaining the external radius, which ensures that the space taken up by the fuel rods remains unchanged. Additionally, the fuel pellet radius has been increased to maintain the same gap width. This approach was firstly proposed and adopted in the IAEA Coordinated Research Project (CRP) ACTOF and then, the same approach was considered in the latest ATF-related IAEA CRP project known as ATF-TS.

This VVER-1000 model for the TRACEV5P6 system code has been validated in steady state conditions against data from a VVER-1000/V320 NPP. The values obtained with the TRACEV5P6 system code are very close to the reference plant data, see Table 1. It should be noted that the steady state of the model remains unchanged when the cladding is modified to FeCrAl or Cr-coated Zry. Only small changes are found in the fuel temperatures because of the pellet diameter increase.

#### 4. Station Blackout sequence

The first analyzed scenario is an SBO sequence, comparing the impact of both ATF claddings under consideration with the conventional E110 cladding. This analysis is based on the assumption that there is no

Table 1  
Steady State parameters of the VVER-1000 TRACE5P6 model.

Parameter	Reference NPP (Kolev et al., 2006)	TRACEV5P6
Core power [MW]	3010	3010
Core outlet pressure [MPa]	15.70	15.74
PZR level [m]	8.70	8.71
CLs temperature [K]	560.85	560.96
HLs temperature [K]	591.55	591.13
Average loop mass flowrate [kg/s]	4456	4457
SG outlet pressure [MPa]	6.27	6.27
MFW mass flowrate [kg/s]	409	408
MFW temperature [K]	493	493
SG level [m]	2.50	2.50

restoration of external power or recovery of any emergency diesel generator, resulting in the unavailability of the MFW, AFW and EFW during the whole SBO sequence.

During the first one and a half hours of the sequence, the Reactor Coolant System (RCS) inventory is cooled by means of the SGs. Consequently, the level on the secondary side of the SGs drops as the water inventory boils off. When the secondary side of the SGs is low, the pressure in the RCS begins to rise until it reaches the set point for the PZR safety valves. At this point, the RCS inventory begins to decrease due to the lost inventory through the safety valves, see Fig. 5. Table 2 shows the main events of the SBO sequence for the three simulations performed for the three types of cladding under study.

The results show that the temperature of 1477 K is reached after 13846 s of simulation for the E110 cladding, 16341 s for the Cr-coated cladding and 16506 s for the FeCrAl cladding. Besides, the eutectic temperature for the Cr-coated Zry (1605.15 K) is exceeded after 16736 s and the melting temperature for the FeCrAl (1773 K) is reached after 17686 s, see Fig. 6.

Furthermore, in the case of Cr-coated Zry, the simulation shows a sudden change in trend, causing the PCT to rise rapidly once it reaches

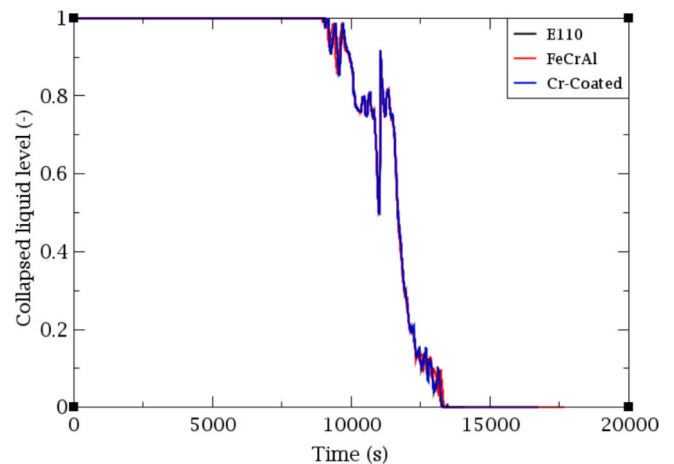


Fig. 5. Core collapsed liquid level, Station Blackout sequence.

**Table 2**  
Station Blackout sequence events.

Event	E110 [s]	Cr-coated [s]	FeCrAl [s]
SBO (SCRAM, MFW pump and MCPs trip, TT, loss of the condenser)	300	300	300
BRU-A valves open (P <sub>SL</sub> > 7.25 MPa)	310	310	310
PZR safety valves begin to cycle (P <sub>PZR</sub> > 18.13 MPa)	5120	5120	5055
SGs secondary side empty	7910	7963	7845
Collapsed liquid level in the core starts to decrease	8901	8900	8921
Core uncovered	11,706	11,711	11,711
PCT > 1477 K	13,846	16,341	16,506
PCT Cr-coated Zry > 1605 K	–	16,736	–
PCT FeCrAl > 1773 K	–	–	17,686

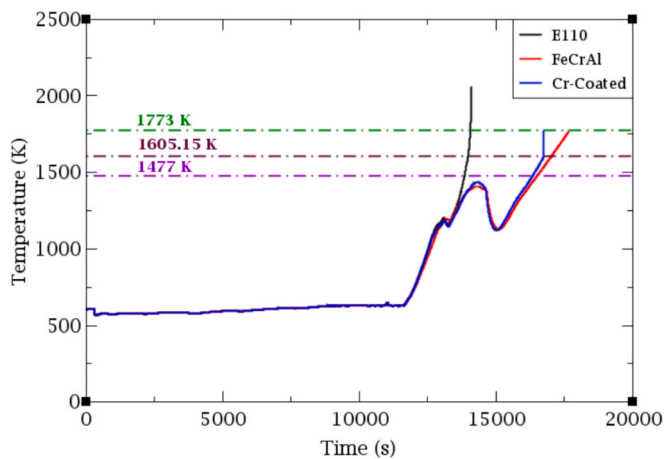


Fig. 6. Peak Cladding Temperature, Station Blackout sequence.

1605.15 K. This is because the eutectic reaction between the Zr and Cr begins at this temperature, which accelerates cladding oxidation.

Thus, the analysis demonstrates that the new ATF claddings could significantly improve the time margin, offering an additional 41 to 64 min for the corresponding human actions required to remove residual heat. This could be critical in avoiding severe accident scenarios.

**5. Large break LOCA sequence**

Two Double Ended Guillotine Break (DEGB) LOCA sequences with different ECCS configurations, which were previously analyzed in (Redondo-Valero et al., 2023a), were considered:

- 1st case: LBLOCA safety systems Success Criteria (SC) (Skalozubov et al., 2010), i.e., availability of 2 out of 3 HPIS trains and 2 out of 4 HA-1 trains.
- 2nd case: LBLOCA along with SBO, i.e., and 4 out of 4 HA-1 are available.

In the LBLOCA case considering the SC for the ECCSs (see Table 3 and Fig. 7 and Fig. 8), it can be observed that even though the HPIS is injected within seconds after the LBLOCA, it cannot counteract the inventory loss through the break. This leads to the core uncovering and later a high PCT value within the first hundred seconds of the simulation. The results also show that the PCT considering FeCrAl cladding is almost 300 K lower than those obtained for E110 and Cr-coated Zry cladding.

The LBLOCA sequence coincident with a SBO (Table 3 and Fig. 9 and

**Table 3**  
DEGB LBLOCA sequences events.

Event	Success criteria ECCS configuration			No active ECCS		
	E110 [s]	Cr-coated [s]	FeCrAl [s]	E110 [s]	Cr-coated [s]	FeCrAl [s]
DEGB-LBLOCA	300	300	300	300	300	300
SCRAM signal (Power > 2250 MW and P <sub>core</sub> < 14.7 MPa) and TT and MFW pumps shutdown signal (P <sub>HL</sub> < 14.7 MPa)	301	301	301	301	301	301
Start of the CRAs insertion (signal + delay)	303	303	303	303	303	303
HPIS injection (P <sub>RCS</sub> < 10.78 MPa and T <sub>sat</sub> - T <sub>HL</sub> < 10 K)	304	304	304	–	–	–
Start of HA-1 and HA-4 injection (P <sub>RCS</sub> < 6.07 MPa)	306	306	306	306	306	306
MCPs coast-down begins (SG level < 2 m)	312	312	312	313	313	313
TT (signal + delay + turbine closing time)	315	315	315	315	315	315
MFW pumps trip/EFW pumps start-up (signal + delay)	340	340	340	340	340	340
PCT > 1477 K	–	–	–	377	390	407
PCT Cr-coated Zry > 1605 K	–	–	–	–	413	–
PCT FeCrAl > 1773 K	–	–	–	–	–	505
Core reflooding ends	822	904	882	–	–	–

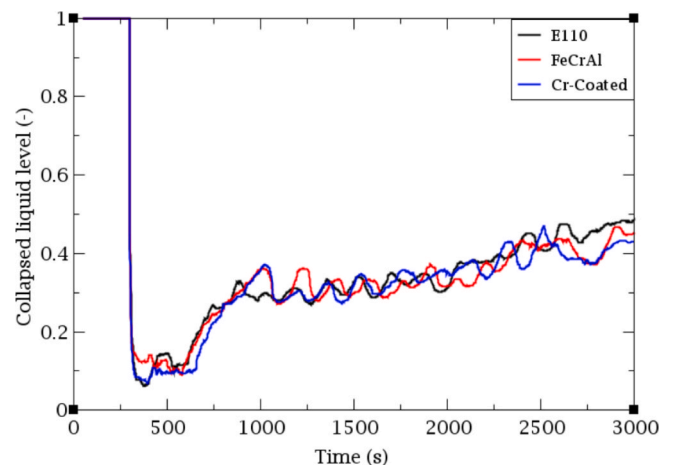


Fig. 7. Core collapsed liquid level, DEGB LBLOCA (success criteria ECCS configuration) sequence.

Fig. 10), it is observed that the AC are exceeded within the first minutes of the sequences. This is due to the fact that the RCS inventory cannot be replenished by any safety system once the HA-1 have been discharged. The simulations considering the ATFs cladding show that the AC are exceeded about 100 s later for the FeCrAl cladding (considering 1773 K as AC) and 80 s later for the Cr-coated Zry (considering 1605.15 K as

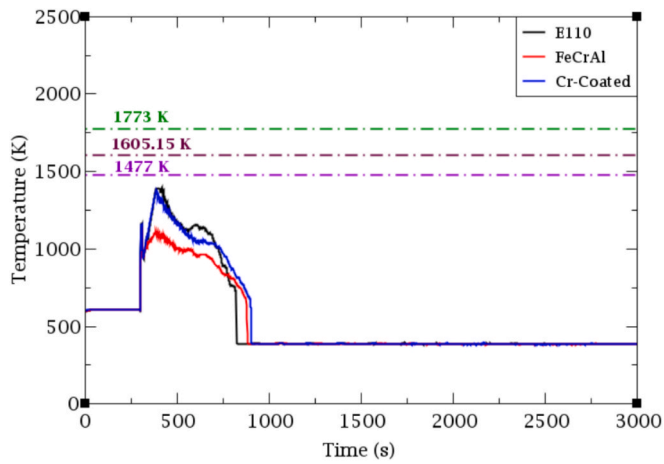


Fig. 8. Peak Cladding Temperature, DEGB LBLOCA (success criteria ECCS configuration) sequence.

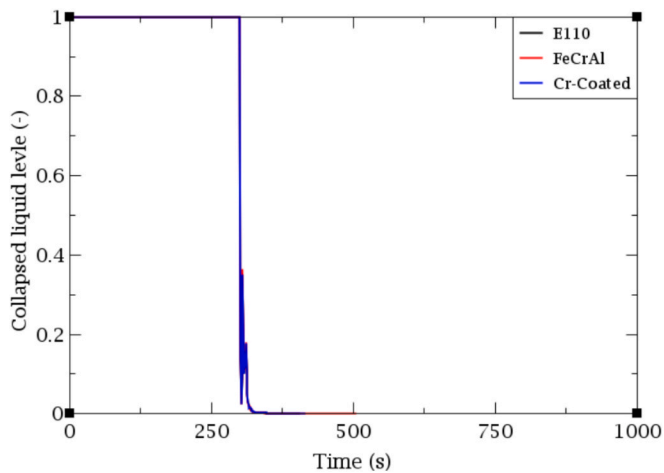


Fig. 9. Core collapsed liquid level, DEGB LBLOCA (no active ECCS) sequence.

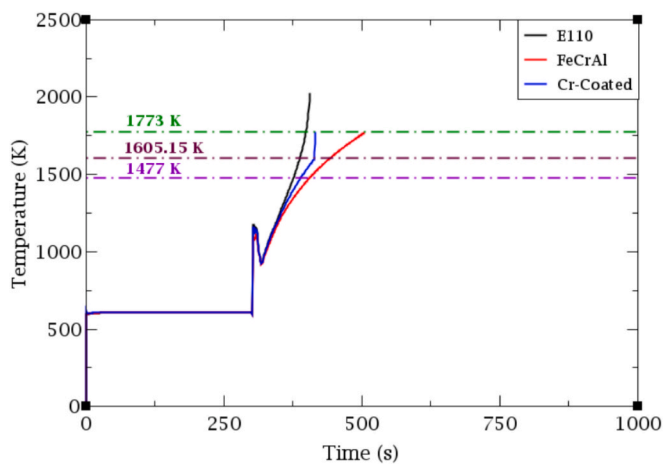


Fig. 10. Peak Cladding Temperature, DEGB LBLOCA (no active ECCS) sequence.

AC).

### 6. SBLOCA sequence with the failure of the HPIS

In previous analyses, see (Redondo-Valero et al., 2024), it was observed that the SBLOCA sequences reach successful end states with the only actuation of 1 out of 3 HPIS trains, achieving very low values for the PCT. However, if the HPIS is not available, some SBLOCA sequences reach CD despite the full availability of the HA-1 and the LPIS. This is because the pressure in the RCS remains above the HA-1 and LPIS set points, preventing the systems from injecting water into the RCS before the PCT reaches the AC.

Two SBLOCA sequences with break sizes of 1 and 2 in. and HPIS failure have been selected for analysis considering the FeCrAl and Cr-coated Zry claddings. In these sequences, it has been assumed that the LPIS and HA-1 trains available are those that meet the SC: 1 out of 3 LPIS trains and 2 out of 4 HA-1 trains (Skalozubov et al., 2010).

For the 1-inch SBLOCA, the simulations have shown that the time margin provided by both ATF materials is insufficient to allow the RCS pressure to reach the LPIS setpoint. This prevents reflooding of the core before the PCT exceeds 1477 K, see Fig. 11 and Fig. 12 and Table 4.

Conversely, the simulation results for the 2-inch SBLOCA case indicate that reflooding of the core occurs before the PCT reaches the AC for both the FeCrAl and Cr-coated Zr claddings, see Fig. 13 and Fig. 14 and Table 4.

In addition, simulations have been performed to consider other break sizes involving HPIS failure, with break diameter increments of 0.25 in. and different cladding materials. Damage curves have been constructed for each cladding material from these simulations, providing information on the time at which AC are reached in each case, see Fig. 15. The obtained damage curves show:

- From 2.25 in. onwards, the SBLOCA with HPIS failure reaches a success end state for all cladding material.
- In the 2 in. break, AC is reached only when E110 cladding is considered, but not when any ATF claddings is considered.
- In the 1.75 in. break AC is achieved for the FeCrAl cladding when the AC temperature is considered to be 1477 K, but not when it is considered to be 1773 K. In addition, AC is exceeded for both Cr-coated Zry AC (1477 K and 1605 K).
- Between 1 and 1.5 in. AC are exceeded for all cladding materials.

### 7. Summary of Core damage time for E100, FeCrAl and Cr-Coated Zry claddings

This section compares the CD times (corresponding to the time to

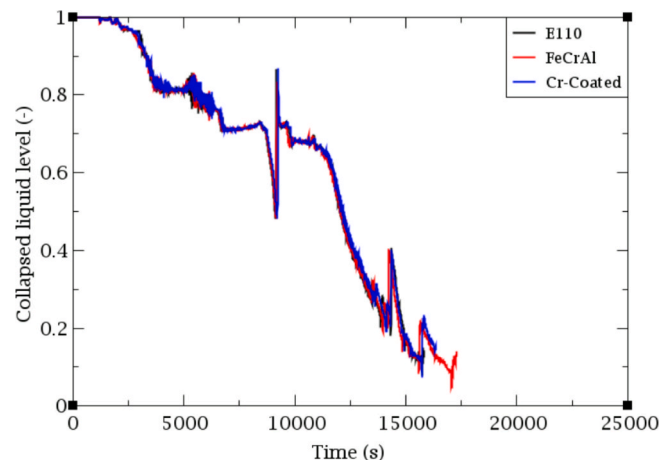


Fig. 11. Core collapsed liquid level, SBLOCA (1 in.) sequence.

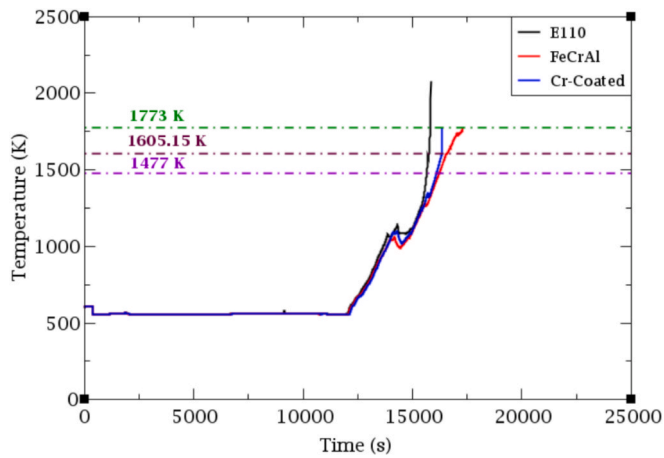


Fig. 12. Peak Cladding temperature, SBLOCA (1 in.) sequence.

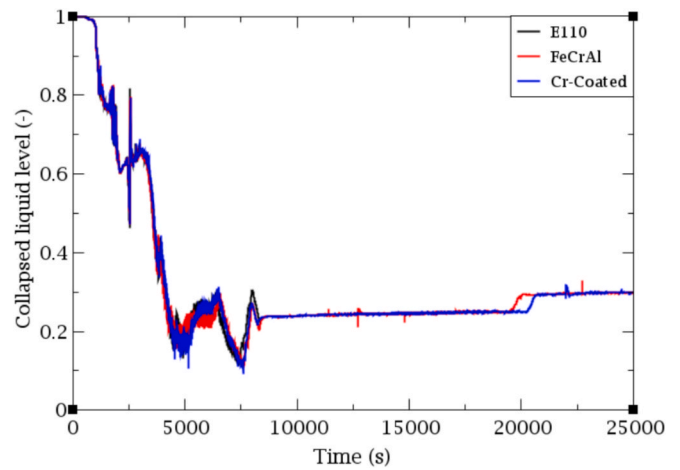


Fig. 13. Core collapsed liquid level, SBLOCA (2 in.) sequence.

Table 4  
SBLOCA sequences events.

Event	SBLOCA – 1 in.			SBLOCA – 2 in.		
	E110 [s]	Cr-coated [s]	FeCrAl [s]	E110 [s]	Cr-coated [s]	FeCrAl [s]
SBLOCA	300	300	300	300	300	300
SCRAM signal (Power > 2250 MW and $P_{core} < 14.7$ MPa) and TT and MFW pumps shutdown signal ( $P_{HL} < 14.7$ MPa)	365	365	365	315	315	315
Start of the CRAs insertion (signal + delay)	367	367	367	317	317	317
TT (signal + delay + turbine closing time)	380	380	380	330	330	330
MFW pumps trip/ EFW pumps start-up (signal + delay)	405	405	405	355	355	355
MCPs coast-down begins (SG level > 2.75 m)	995	995	995	1030	1030	1030
Start of HA-1 and HA-4 injection ( $P_{RCS} < 6.07$ MPa)	14,307	14,297	14,187	3820	3845	3775
LPIS injection ( $P_{RCS} < 2.55$ MPa and $T_{sat} - T_{HL} < 10$ K)	–	–	–	7726	7752	7812
PCT > 1477 K	15,657	16,102	16,227	8122	–	–
PCT Cr-coated Zry > 1605 K	–	16,332	–	–	–	–
PCT FeCrAl > 1773 K	–	–	17,308	–	–	–
Core reflooding ends	–	–	–	>	>	>
				25,000	25,000	25,000

exceed the AC) for the two advanced cladding materials analyzed – FeCrAl and Cr-coated Zry – over the SBO, LBLOCA and SBLOCA sequences with respect to E110. The differences in CD times between E110, Cr-coated Zry and FeCrAl cladding are shown in Table 5 and Table 6.

The most significant impact of ATF implementation is observed in

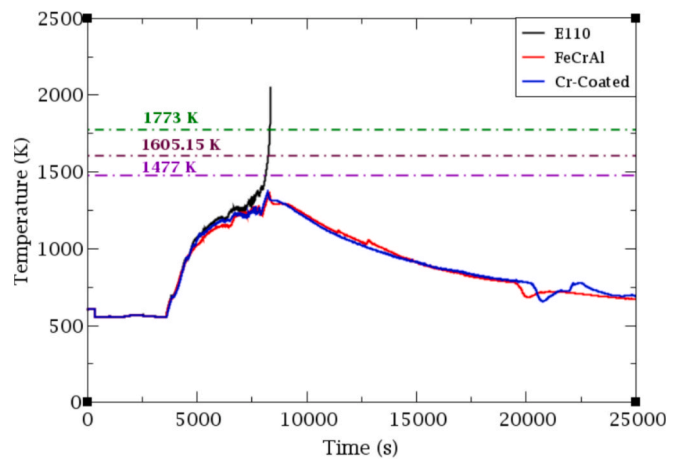


Fig. 14. Peak Cladding Temperature, SBLOCA (2 in.) sequence.

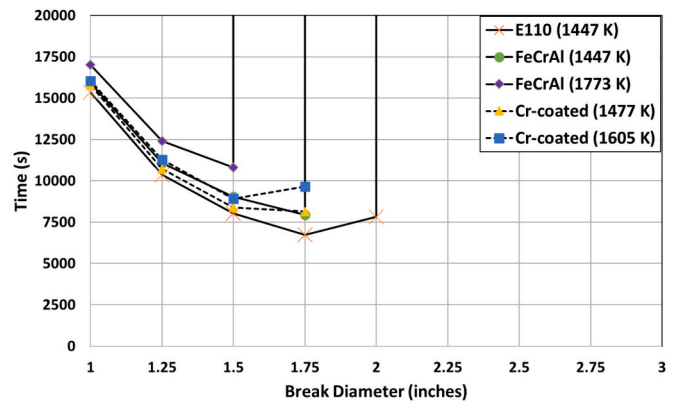


Fig. 15. Damage curve for SBLOCA with HPIS failure.

the 2-inch SBLOCA sequence, where the replacement of E110 with ATF cladding transforms a CD sequence into a successful one. Moreover, in the SBO sequence, the ATFs provide a significant time margin, exceeding 40 min for Cr-coated Zry and over an hour for FeCrAl. However, in the LOCA-DEGB sequence without active ECCS actuation, the ATF implementation provides little to no additional time margin. Globally, the potential implementation of ATF in light water reactors (such as the VVER-1000) is recognised as having the capacity to increase of safety margins and time available for human actions in several accidental

**Table 5**

Core damage time (since the beginning of the accidental sequences) comparison for Cr-Coated Zry vs. E110.

Sequence	E110 (1477 K) [s]	Cr-coated Zry (1477 K) [s] ( $\Delta t$ ) [min]	Cr-coated Zry (1605 K) [s] ( $\Delta t$ ) [min]
2 in. SBLOCA	7822	No damage	No damage
1 in. SBLOCA	15,357	15,802 (7.5)	16,032 (11)
DEGB LBLOCA (No active ECCS)	77	90 (0.2)	113 (0.5)
SBO	13,546	16,041 (41.5)	16,436 (48)

**Table 6**

Core damage time (since the beginning of the accidental sequences) comparison for FeCrAl vs. E110.

Sequence	E110 (1477 K) [s]	FeCrAl (1477 K) [s] ( $\Delta t$ ) [min]	FeCrAl (1773 K) [s] ( $\Delta t$ ) [min]
2 in. SBLOCA	7822	No damage	No damage
1 in. SBLOCA	15,357	15,927 (9.5)	17,008 (27.5)
DEGB LBLOCA (No active ECCS)	77	107 (0.5)	205 (2)
SBO	13,546	16,206 (44)	17,386 (64)

sequences.

## 8. Conclusions

In the present work, a series of accidental scenarios, including SBLOCA, LBLOCA and SBO sequences, have been simulated with in-house TRACEP6 versions capable of modeling ATF, with the aim of analyzing the increase of safety margins and time available provided by the implementation of the FeCrAl and the Cr-coated Zry cladding material in a VVER-1000 reactor. The main conclusions obtained are as follows:

- SBO sequence: Using ATFs increased the time available significantly to over 40 min for Cr-coated Zry and over one hour for FeCrAl material, providing an advantage for potential main control room crew intervention or systems recovery.
- LBLOCA sequence: The use of FeCrAl provides an improvement in PCT safety margin when active ECCS are available. Moreover, in the case of LBLOCA coinciding with SBO, FeCrAl and Cr-coated Zry delay the core damage time compared to E110, but the increase of time available remains relatively short.
- SBLOCA sequences without HPIS: In general, for sequences with breaks of less than 2 in., the time available to implement accident management strategies is increased. In particular, for the 2 in. SBLOCA, the use of FeCrAl and Cr-coated Zry transforms a core damage sequence into a successful sequence.

As a final remark, it is crucial to establish which are the adequate acceptance criteria for FeCrAl and Cr-coated Zry claddings, as the time margin differences obtained between the both criteria under discussion for each ATF cladding material, are significant.

### CRedit authorship contribution statement

**Elena Redondo-Valero:** Writing – review & editing, Writing – original draft, Methodology, Investigation, Formal analysis,

Conceptualization. **Cesar Queral:** Writing – review & editing, Writing – original draft, Supervision, Methodology, Investigation, Funding acquisition, Formal analysis, Conceptualization. **Kevin Fernandez-Cosials:** Writing – review & editing, Writing – original draft, Methodology, Investigation, Formal analysis, Conceptualization. **Jorge Sanchez-Torrijos:** Writing – review & editing, Writing – original draft, Methodology, Investigation, Formal analysis, Conceptualization. **David Canal:** Writing – review & editing, Writing – original draft, Methodology, Investigation, Formal analysis, Conceptualization. **Emilio Castro-Gonzalez:** Writing – review & editing, Writing – original draft, Methodology, Formal analysis, Conceptualization. **Victor Hugo Sanchez-Espinoza:** Writing – review & editing, Writing – original draft, Methodology, Formal analysis, Conceptualization.

### Declaration of competing interest

The authors declare that they have no known competing financial interests or personal relationships that could have appeared to influence the work reported in this paper.

### Acknowledgement

UPM Nuclear Safety group acknowledges technical and financial support granted in the framework of the project “SUBV-16/2021 Safety Margins increase in LWR by means of Accident Tolerant Fuel (ATF)” funded by the Spanish Nuclear Safety Council (CSN).

### Data availability

The authors do not have permission to share data.

### References

- Aragon, P., Fera, F., Herranz, L.E., Schubert, A., Van-Uffelen, P., 2025. Fuel performance modelling of Cr-Coated Zircaloy under DBA/LOCA conditions. *Ann. Nucl. Energy* 211. <https://doi.org/10.1016/j.anucene.2024.110950>.
- Baker, U., Choi, Y.J., Rollins, N., Nguyen, K., Jung, W., Whitmeyer, A., Hou, J., Lindley, B., 2024. Source term analysis of FeCrAl accident tolerant fuel using MELCOR. *Ann. Nucl. Energy* 202. <https://doi.org/10.1016/j.anucene.2024.110482>.
- Brachet, J.C., Rouesne, E., Ribis, J., Guilbert, T., Urvoy, S., Nony, G., Toffolon-Maslet, C., Le Saux, M., Chaabane, N., Palancher, H., David, A., Bischoff, J., Augereau, J., Pouillier, E., 2020. High temperature steam oxidation of chromium-coated zirconium-based alloys: Kinetics and process. *Corros. Sci.* 167. <https://doi.org/10.1016/j.corsci.2020.108537>.
- Canal, D., Queral, C., Castro, E., Sanchez-Torrijos, J., 2025. Analysis of the time available in case of accidental TLFW sequences in PWR NPPs with ATF, in: American Nuclear Society Annual Conference. Chicago, IL, United States.
- Doncel, N., Martinez, L., Aragon, P., Fera, F., Herranz, L.E., Queral, C., Fernandez, K., Ruiz-Hervias, J., Cristobal-Beneyto, M., Castro, E., Sanchez-Torrijos, J., Soles, A., 2024. R&D in advanced technology fuels (ATFs) in Spain. *Nuclear Engineering and Design* 424. <https://doi.org/10.1016/j.nucengdes.2024.113246>.
- Field, K.G., Snead, M.A., Yamamoto, Y., Terrani, K.A., 2018. Handbook on the Material Properties of FeCrAl Alloys for Nuclear Power Production Applications, ORNL/SPR-2018/905 Rev. 1.
- IAEA, 2020. Analysis of Options and Experimental Examination on Fuels for Water Cooled Reactors with Increased Accident Tolerance (ACTOF), IAEA-TECDOC-1921.
- Kolev, N., Petrov, N., Donovan, J., Angelova, D., Aniel, S., Royer, E., Nikonov, S., 2006. VVER-1000 Coolant Transient Benchmark - Phase 2 (V1000CT-2). Vol. 11: MSLB Problem - Final Specifications, Phase. MSLB Problem - Final Specifications.
- Queral, C., Sánchez-Espinoza, V., Egelkraut, D., Fernández-Cosials, K., Redondo-Valero, E., García-Morillo, A., 2021. Safety Systems of Gen-III/Gen-III+ VVER reactors. *Nuclear España*.
- Redondo-Valero, E., Queral, C., Fernandez-Cosials, K., Sanchez-Espinoza, V., 2023a. Analysis of MBLOCA and LBLOCA success criteria in VVER-1000/V320 reactors: New proposals for PSA Level 1. *Nucl. Eng. Technol.* 55, 623–639.
- Redondo-Valero, E., Queral, C., Fernandez-Cosials, K., Sanchez-Espinoza, V., 2023b. Safety margins improvement by means of the passive second stage hydroaccumulators in a VVER-1000/V320 reactor. *Nucl. Eng. Des.* 414.
- Redondo-Valero, E., Queral, C., Fernandez-Cosials, K., Sanchez-Espinoza, V.H., Sanchez-Perea, M., Groudev, P., 2024. Management of the SBLOCA sequences with HPIS failure in VVER-1000/V320 reactors; comparison with Westinghouse PWR strategies, 177, 105414. *Progress in Nuclear Energy*. <https://doi.org/10.1016/j.pnucene.2024.105414>.
- Redondo-Valero, E., Queral, C., Fernandez-Cosials, K., Sanchez-Espinoza, V.H., 2025. Safety margins improvement by means of the passive heat removal system and the

- HA-2 in VVER-1000/V320 reactors, 178, 105825. *Prog. Nucl. Energy*. <https://doi.org/10.1016/j.pnucene.2025.105825>.
- Sanchez-Espinoza, V., Bottcher, M., 2006. Investigations of the VVER-1000 coolant transient benchmark phase with the coupled system code RELAP5/PARCS. *Progress in Nuclear Energy*, Progress in Nuclear Energy 48, 865–879. <https://doi.org/10.1016/j.pnucene.2006.06.004>.
- Sanchez-Torrijos, J., 2024. Assessment of safety issues in NuScale and Gen II PWR under accident conditions using TRACE, PhD Thesis. Universidad Politécnica de Madrid (2024).
- Sanchez-Torrijos, J., Soler, A., Castro, E., Canal, D., Queral, C., 2024. Simulation of the Halden IFA 650.10 LOCA test considering conventional and advanced cladding materials using TRACE, in: *TopFuel*. Grenoble, France.
- Skalozubov, B., Klyuchnikov, A., Kolykhanov, B., 2010. Fundamentals of management of design accidents with loss of coolant at the power plant (in Russian). National Academy of Sciences of Ukraine, Institute of NPP Safety Problems. - Chernobyl (Kiev region): Institute of NPP Safety Issues, 2010. ISBN 978-966-02-5203-5.
- Wu, S., Shirvan, K., 2020. System code evaluation of near-term accident tolerant claddings during boiling water reactor short-term and long-term station blackout accidents. *Nuclear Engineering and Design* 356. <https://doi.org/10.1016/j.nucengdes.2019.110362>.
- Yue, J., Xu, W., Koroush, S., 2020. System code evaluation of near-term accident tolerant claddings during pressurized water reactor station blackout accidents. *Nuclear Engineering and Design* 368. <https://doi.org/10.1016/j.nucengdes.2020.110814>.
- Zhang, J., Xu, P., Sevecek, M., Sim, K.S., Khaperskaia, A., 2014. Contribution of IAEA coordinated research projects to light water reactors advanced technology fuel testing and simulation. *Nuclear Engineering and Design* 418. <https://doi.org/10.1016/j.nucengdes.2024.112910>.